IEEE Access
Multidisciplinary | Rapid Review | Open Access Journal

Received March 22, 2020, accepted April 24, 2020, date of publication May 6, 2020, date of current version May 18, 2020.

Digital Object Identifier 10.1109/ACCESS.2020.2991727

Fractional Distance Regularized Level Set Evolution With Its Application to Image Segmentation

MENG LI[1,2], YI ZHAN[1,2], AND YONGXIN GE[3]
[1]College of Mathematics and Statistics, Chongqing Technology and Business University, Chongqing 400067, China
[2]Chongqing Key Laboratory of Social Economy and Applied Statistics, Chongqing 400067, China
[3]School of Big Data and Software Engineering, Chongqing University, Chongqing 401331, China

Corresponding author: Yongxin Ge (yongxinge@cqu.edu.cn)

This work was supported in part by the National Natural Science Foundation of China under Grant 61772093, in part by the Chongqing Research Program of Basic Science and Frontier Technology under Grant cstc2018jcyjAX0410, and in part by the Fundamental Research Funds for the Central Universities under Grant 2019CDYGYB014, Grant 2019CDCGRJ217, and Grant 2019CDXYRJ0011.

ABSTRACT To avoid the irregularities during the level set evolution, a fractional distance regularized variational model is proposed for image segmentation. We first define a fractional distance regularization term which punishes the deviation of the level set function (LSF) and the signed distance function. Since the fractional derivative of the constant value function outside the starting point is nonzero, the fractional gradient modular of the LSF does not approach infinity where the integer order gradient modular is close to 0. This prevents the sharp reverse diffusion of LSF in flat areas and ensures the smooth evolution of LSF. Then, we use the Grünwald-Letnikov (G-L) fractional derivative to derive the discrete forms of the conjugate of fractional derivatives and fractional divergence. To facilitate the calculation of fractional derivatives and their conjugates, we designed their covering templates. Finally, a numerical solution to the minimization of the energy functional is obtained from these discrete forms and covering templates. Numerical experiments of medical images with different modalities show that the model in this paper can well segment weak images and intensity inhomogeneity images.

INDEX TERMS Image segmentation, fractional distance regularization, level set evolution, fractional derivative, fractional divergence.

I. INTRODUCTION

Image segmentation is a crucial step in image processing and computer vision, and also a difficult task. The main reason is that various complex factors in nature determine the diversity of images. For example, medical images have characteristics such as strong noise, blur, and intensity inhomogeneity. Infrared images have features such as complex backgrounds and changing backgrounds. These features make image segmentation particularly difficult. For a long time, researchers have conducted a lot of research using various tools and proposed various segmentation methods, including threshold method, region segmentation, Laplace operator edge detection, wavelet transform, random algorithm, graph cut, and level set segmentation methods, etc. Among them, the level set method is a non-linear image segmentation method introduced by Osher and Sethian [1] in 1987. They implicitly describe the evolution curve as the zero level set of the high-dimensional level set function (LSF), using the nature of the image and the geometric properties of the LSF to design a variational model or partial differential equation (PDE). By minimizing the energy of the variational model or solving the PDE, the zero level curve is constrained to move toward the target edge, thereby characterizing the target edge. The level set method applied to image segmentation has great advantages. The LSF is always designed as a simple function on a fixed grid, which is convenient for numerical calculations. Moreover, the LSF can automatically and flexibly deal with the topological structure changes of the zero level curve during the level set evolution, such as rupture, merge, etc. Therefore, it is widely used for various image segmentation [2]–[4], especially for medical images with inhomogeneity and noisy infrared images.

The associate editor coordinating the review of this manuscript and approving it for publication was Jenny Mahoney.

However, in these level set methods the LSF typically develops irregularities, which will cause its numerical errors and destroy the stability of the level set evolution. To solve this problem, Caselles *et al.* [5] periodically initializes the LSF as a signed distance function to maintain the stability of the evolution of the LSF. The numerical implementation of this method is very time-consuming, which limits its use in infrared targets tracking and other real-time applications. Later, Li *et al.* [6] designed the distance regularization term to directly penalize the deviation of the LSF and the signed distance function from the perspective of energy functional, which greatly improved the computing efficiency. However, this will lead to the sharp change of the LSF in a flat area, which affects the image segmentation results. Li *et al.* [7], Wang *et al.* [8], and Wang *et al.* [9] constructed different double-well potential functions for distance regularization, to a certain extent, avoiding sharp changes in flat regions. But the improved model will make the gradient modular in the smaller slope area approach 0, which is in contradiction with that the LSF always approximates as a signed distance function.

Fractional calculus is an important branch of mathematics. It was born in 1695 and appeared almost at the same time as classical integer order calculus. However, its development was much slower than integer order calculus. In the past three centuries, its research has focused on the purely theoretical field of mathematics. With the gradual development and improvement of the theory, it has been found that fractional calculus can describe many non-classical phenomena in the natural sciences and engineering applications that can not be described by integer order derivatives or integrals. In recent decades, fractional differential equations and fractional PDEs have been widely used to describe problems in optical and thermal systems, rheology, materials and mechanical systems, signal processing and system identification, control, robotics and other applications. In fact, everything in nature (including image pixels) often has a large autocorrelation. Fractional derivative can naturally describe the fractal geometric features such as the texture of the image. Naturally, fractional calculus is also applied to image processing. Up to now, fractional calculus has been widely applied in many areas, especially in the field of image processing [10–16]. Pu *et al.* [10, 11] intended to implement a class of fractional differential masks with high-precision for multiscale texture enhancement. Zhang *et al.* [12] proposed a novel fuzzy subpixel fractional partial difference for ultrasound speckle reduction. Zhang and Wei [13] defined a new space of functions of fractional-order bounded variation and proposed a class of fractional-order multiscale variational models for image denoising. Chen *et al.* [14] integrated fractional differentiation, fractional gradient magnitude, and difference image information into the well-known local Chan-Vese model for image segmentation. Ren [15] presented an image up-sampling algorithm based on fractional-order bidirectional diffusion. Laghrib *et al.* [16] gave a nonconvex fractional variational model for multi-frame image super-resolution. The fractional calculus has many advantages for image processing. The enhancement and preservation of complex texture details in the smooth area by fractional differential-based approach appear obvious better than by traditional integral-based algorithms [10]. It has many methods that can define the fractional calculus such as Riemann-Liouville fractional calculus, and Grünwald-Letnikov fractional calculus. The fractional calculus is a nonlinear operator. Its nonlinear and nonlocal properties are very effective for image processing.

In order to solve the problem of irregularities during the level set evolution, we put forward a fractional distance regularized variational model for image segmentation. The work of this paper includes the following parts. First, considering the non-local nature of the fractional derivative, a fractional distance regularization term is proposed. It penalizes the deviation of the LSF and the signed distance function by minimizing the corresponding energy functional and keeps inherent regularity of the LSF in the evolution. Secondly, utilizing the Grünwald-Letnikov fractional derivative and the inner product of L_2 space, the conjugate of the fractional derivative and the discrete form of fractional divergence are derived. Third, since the fractional distance regularization term does not contain image information, this term can be combined with any external energy term based on image information to achieve artificial or natural image segmentation. To this end, we design an external energy term based on the image edge stop function and Laplace operator, and combine it with a fractional distance regularization term to form a total energy functional. Among them, the external energy term forces the zero level curve to automatically generate and characterize the edges of the image during the level set evolution, and the fractional regularization term guarantees the smooth change of the LSF. Finally, we give the discrete covering template of the fractional derivative and its conjugate to obtain a numerical solution for minimizing the energy functional. Experiments show the effectiveness of the model in this paper. It makes the LSF evolve smoothly and can better constrain the LSF to segment noisy and weak target medical images with intensity inhomogeneity.

The remainder of the paper is organized as follows: In Section II, we give some preliminaries: the fractional derivative and the distance regularized level set evolution for image segmentation. In Section III, the new fractional distance regularized variational model for image segmentation model is proposed. In Section IV, we obtain a numerical solution by minimizing the energy functional. Experiment results are shown in Section V. Finally, we conclude our paper in Section VI.

II. BACKGROUND

A. DEFINITION OF FRACTIONAL DERIVATIVE

As a generalization of the integer order derivative, the fractional derivative has a long history, but until now there is no uniform definition. The commonly used [17], [18] are

the Grünwald-Letnikov definition, the Riemann-Liouville definition and the Caputo definition. This article selects the Grünwald-Letnikov definition. For any real number υ, assuming that the function $s(x)$ is continuously differentiable for any $x \in R$ and a is real constant, the υth fractional derivative is defined as [18]

$$
\begin{aligned}
{}_aD_x^{\upsilon} s(x) &= \lim_{\substack{h \to 0 \\ Nh = x-a}} h^{-\upsilon} \sum_{k=0}^{N-1} (-1)^k \binom{\upsilon}{k} \cdot s(x - kh) \\
&= \lim_{N \to \infty} \frac{h^{-\upsilon}}{\Gamma(-\upsilon)} \sum_{k=0}^{N-1} \frac{\Gamma(k-\upsilon)}{\Gamma(k+1)} \cdot s(x - kh), \qquad (1)
\end{aligned}
$$

where $\Gamma(x)$ is a Gamma function. For convenience, ${}_aD_x^{\upsilon} s(x)$ is abbreviated as $D^{\upsilon} s(x)$. When $s(x)$ is a constant C, we may have

$$
D^{\upsilon} C = \frac{(x-a)^{-\upsilon}}{\Gamma(1-\upsilon)}.
$$

For all $x \neq a$, we have $D^{\upsilon} C \neq 0$. If the variable x is regarded as time, the fractional derivative reflects the "memory dependence on time" at the $x - kh$ time, and x as the position, reflects the "memory dependence on positon" at the $x - kh$ position, so the fractional derivative has nonlocal nature.

In the beginning, the research of fractional calculus was mainly concentrated on the field of pure theory [17], [18]. In practical applications, researchers have gradually discovered that the geometric meaning of the fractional derivative is the fractional slope of the function curve, and the physical meaning is a continuous fractional measure of speed and distance in the direction of change [19]. Fractional differential equations are very suitable for characterizing materials and processes with memory and genetic properties. Thus it becomes an important tool for mathematical modeling of complex mechanics and physical processes [20]. Since it can cause non-linear changes in the image field, it is widely used in image processing.

B. DISTANCE REGULARIZED VARIATIONAL LEVEL SET IMAGE SEGMENTATION MODEL

In image segmentation, to make the LSF evolve smoothly, it is often necessary to initialize and periodically re-initialize the LSF as a signed distance function. The traditional level set image segmentation method [5] is to force the LSF to approximate the signed distance function by repeatedly solving the following PDE

$$
\frac{\partial \phi}{\partial t} = sign(\psi)(1 - |\nabla \phi|),
$$

where ψ is a function that is repeatedly initialized, and $sign(\cdot)$ is a signum function. The repetitive process of solving and initializing is very time-consuming and labor-intensive, which severely limits its application in practice. In addition, when ψ is not smooth, the LSF ϕ will gradually deviate from the signed distance function during the evolution process. This means that the theoretical and practical results of the method are inconsistent [21].

From the perspective of energy functionals, Li *et al.* [6] designed the distance regularization term to directly penalize the deviation of the LSF and the signed distance function. Arnold [22] pointed out that the function that satisfies the condition $|\nabla \phi| = 1$ is a signed distance function plus or minus a constant. In turn, the signed distance function satisfies the property $|\nabla \phi| = 1$. From this, Li *et al.* constructed the following energy functional

$$
E_{reg}(\phi) = \int_{\Omega} \frac{1}{2} (|\nabla \phi| - 1)^2 dxdy. \qquad (2)
$$

Among them, Ω is an image domain, and $\phi(x, y)$: $\Omega \to R$ is an LSF defined on the image domain. From the basic principle of the variational method and the gradient descent method, the corresponding evolution equation of $E_{reg}(\phi)$ is

$$
\frac{\partial \phi}{\partial t} = div\left((1 - \frac{1}{|\nabla \phi|}) \nabla \phi \right). \qquad (3)
$$

We denote $d = (1 - 1/|\nabla \phi|)$, which is the diffusion coefficient of equation (3). The evolution process in the artificial time t given by (3) forces the LSF to move in the $|\nabla \phi| = 1$ direction, and the LSF gradually approaches the signed distance function. The advantage of this method is that the LSF does not need to be initialized and be repeatedly initialized as a signed distance function, which avoids the drastic change of the LSF. Moreover, the LSF can be initialized to a binary function, which significantly improves the calculation efficiency of the level set segmentation model. Therefore, many subsequent variational level set models use the distance regularization term $E_{reg}(\phi)$ as the internal energy term to constrain the change of the LSF itself.

However, the distance regularization term still has some problems in practical applications. Obviously, when $|\nabla \phi| \to \infty$, there is $d \to 1$, which means that the LSF can change at a relatively steady speed in the steep slope area. However, when $|\nabla \phi| \to 0$, there is $d \to -\infty$, which causes the LSF to change sharply in a flat region in the reverse direction. This makes the LSF produce spikes or deep valleys and other phenomena, which brings bad or even wrong segmentation results.

To overcome this problem and obtain better image segmentation, Li *et al.* [6] proposed an external energy term based on the weighted length and weighted area, namely

$$
\begin{aligned}
E_{ext}(\phi) &= \lambda L_g(\phi) + \nu A_g(\phi) \\
&= \lambda \int_{\Omega} g(|\nabla I_{\sigma}|) \delta_{\varepsilon}(\phi) |\nabla \phi| dxdy \\
&\quad + \nu \int_{\Omega} g(|\nabla I_{\sigma}|) H_{\varepsilon}(-\phi) dxdy, \qquad (4)
\end{aligned}
$$

where $\lambda > 0$, $\nu \in R$, $I(x, y)$: $\Omega \to R$ is an image function, $\delta_{\varepsilon}(\phi)$ and $H_{\varepsilon}(\phi)$ are smooth Diric function and smooth Heaviside function respectively. $I_{\sigma} = G_{\sigma} * I$ is the convolution of a Gaussian kernel with a standard deviation σ and image I.

$|\cdot|$ is the gradient modular, and $g(s) = 1/(1+s^2)$ is the edge stop function. Obviously, at the edge of the image, there is $|\nabla I_\sigma| \to \infty$, then $g(|\nabla I_\sigma|) \to 0$. At this time, the energy functional $E_{ext}(\phi)$ reaches a minimum where the evolution of the LSF stops and the edge information of the image is characterized. Combining (2) with (4), Li *et al.* proposed the level set evolution without reinitialization (LSEWR) model for image segmentation

$$E(\phi) = \mu E_{reg}(\phi) + E_{ext}(\phi), \tag{5}$$

where $\mu > 0$ is a constant. The evolution equation corresponding to equation (5) is

$$\frac{\partial \phi}{\partial t} = \mu div\left((1 - \frac{1}{|\nabla\phi|})\nabla\phi\right) + \lambda\delta_\varepsilon(\phi) div(g(|\nabla I_\sigma|)\frac{\nabla\phi}{|\nabla\phi|}) + \nu\delta_\varepsilon(\phi) g(|\nabla I_\sigma|). \tag{6}$$

III. PROPOSED METHOD

To solve the problem that the distance regularization term causes the level set evolution to change sharply in a flat region, we propose a fractional distance regularized level set model for image segmentation. Since the Euler-Lagrange equation corresponding to the proposed fractional variational model will involve concepts such as fractional gradient, conjugate gradient, and divergence, in this section we first derive the discrete fractional gradient, conjugate, and divergence from the definition of the G-L fractional derivative. Then the level set evolution is constrained by the fractional distance regularization term. Finally, we combine the fractional distance regularization term with external energy to construct a fractional distance regularized variational level set model for image segmentation.

A. CONJUGATE OF FRACTIONAL DERIVATIVE AND FRACTIONAL DIVERGENCE

Since the distance between the pixels in an image is not less than 1, we take the step size $h = 1$ in (1). Using the truncation error, the υth fractional derivative of the unary function $s(x)$ can be approximately expressed as

$$\begin{aligned} D^\upsilon s(x) &\triangleq \frac{1}{\Gamma(-\upsilon)} \sum_{k=0}^{N-1} \frac{\Gamma(k-\upsilon)}{\Gamma(k+1)} \cdot s(x-k) \\ &= \sum_{k=0}^{N-1} \frac{\Gamma(k-\upsilon)}{\Gamma(-\upsilon)\Gamma(k+1)} \cdot s(x-k) \\ &= \sum_{k=0}^{N-1} (-1)^k \binom{\upsilon}{k} \cdot s(x-k), \end{aligned} \tag{7}$$

and with $\binom{\upsilon}{k} = \frac{\upsilon(\upsilon-1)\cdots(\upsilon-k+1)}{k!}$, $k = 1, 2, \cdots, N$.

Therefore, the υth fractional partial derivatives of the LSF ϕ along the x and y directions are defined as

$$\begin{aligned} D_x^\upsilon \phi(x,y) &= \frac{\partial^\upsilon \phi(x,y)}{\partial x^\upsilon} \\ &\triangleq \sum_{k=0}^{N-1} (-1)^k \binom{\upsilon}{k} \cdot \phi(x-k, y), \end{aligned} \tag{8}$$

$$\begin{aligned} D_y^\upsilon \phi(x,y) &= \frac{\partial^\upsilon \phi(x,y)}{\partial y^\upsilon} \\ &\triangleq \sum_{k=0}^{N-1} (-1)^k \binom{\upsilon}{k} \cdot \phi(x, y-k). \end{aligned} \tag{9}$$

The υth fractional gradient of the function ϕ is

$$\nabla^\upsilon \phi = (D_x^\upsilon \phi, D_y^\upsilon \phi)^T.$$

The υth fractional gradient modular of the function ϕ is

$$|\nabla^\upsilon \phi| = \sqrt{(D_x^\upsilon \phi)^2 + (D_y^\upsilon \phi)^2}. \tag{10}$$

Let $D^{\upsilon *}$ be the conjugate of the fractional derivative D^υ. Next, we derive the approximate expression of $D^{\upsilon *}$ through the inner product definition.

For $x(t), y(t) \in L^2(R)$, we have inner product on $L^2(R)$

$$\langle x(x), y(x)\rangle = \int_{-\infty}^{+\infty} x(t)y(t)dt.$$

For $\forall h(x) \in C_0^\infty(\Omega)$, according to inner product above we have

$$\begin{aligned} &\langle h(x), D^\upsilon s(x)\rangle \\ &= \int_{-\infty}^{+\infty} h(x) \cdot D^\upsilon s(x) dx \\ &\triangleq \int_{-\infty}^{+\infty} h(x) \cdot \sum_{k=0}^{N-1} (-1)^k \binom{\upsilon}{k} s(x-k) dx \\ &\overset{x-k=t}{=} \int_{-\infty}^{+\infty} \sum_{k=0}^{N-1} (-1)^k \binom{\upsilon}{k} s(t) \cdot h(t+k) dt \\ &\overset{t=x}{=} \int_{-\infty}^{+\infty} \sum_{k=0}^{N-1} (-1)^k \binom{\upsilon}{k} h(x+k) \cdot s(x)\, dx \\ &= \langle \sum_{k=0}^{N-1} (-1)^k \binom{\upsilon}{k} h(x+k), s(x)\rangle. \end{aligned} \tag{11}$$

Denote

$$D^{\upsilon *} h(t) = \sum_{k=0}^{N-1} (-1)^k \binom{\upsilon}{k} h(t+k), \tag{12}$$

then equation (11) becomes

$$\langle h(x), D^\upsilon s(x)\rangle = \langle D^{\upsilon *} h(x), s(x)\rangle. \tag{13}$$

From the definition of the conjugate, $D^{\upsilon *} h(x)$ is the conjugate of $D^\upsilon h(x)$. Let $D_x^{\upsilon *}$ and $D_y^{\upsilon *}$ be the conjugate operators of

D_x^υ and D_y^υ, respectively. According to (12), the approximate calculations of conjugate operators $D_x^{\upsilon*}$ and $D_y^{\upsilon*}$ are

$$D_x^{\upsilon*}\phi(x,y) = \sum_{k=0}^{N-1}(-1)^k \binom{\upsilon}{k} \phi(x+k,y), \tag{14}$$

$$D_y^{\upsilon*}\phi(x,y) = \sum_{k=0}^{N-1}(-1)^k \binom{\upsilon}{k} \phi(x,y+k). \tag{15}$$

From the gradient vector $\nabla^\upsilon\phi = (D_x^\upsilon\phi, D_y^\upsilon\phi)^T$, we can derive the υth fractional divergence. For $\forall h(x) \in C_0^\infty(\Omega)$, we have

$$\begin{aligned}\langle\nabla^\upsilon\phi, \nabla^\upsilon h\rangle &= \int_{-\infty}^{+\infty} D_x^\upsilon\phi \cdot D_x^\upsilon h dx + \int_{-\infty}^{+\infty} D_y^\upsilon\phi \cdot D_y^\upsilon h dy \\ &= \langle D_x^\upsilon\phi, D_x^\upsilon h\rangle + \langle D_y^\upsilon\phi, D_y^\upsilon h\rangle \\ &= \langle D_x^{\upsilon*}(D_x^\upsilon\phi), h\rangle + \langle D_y^{\upsilon*}(D_y^\upsilon\phi), h\rangle \\ &= \langle D_x^{\upsilon*}(D_x^\upsilon\phi) + D_y^{\upsilon*}(D_y^\upsilon\phi), h\rangle_{L^2}. \end{aligned} \tag{16}$$

Denoting $(-1)^\upsilon div^\upsilon\phi = D_x^{\upsilon*}(D_x^\upsilon\phi) + D_y^{\upsilon*}(D_y^\upsilon\phi)$, by (16) we have

$$\langle\nabla^\upsilon\phi, \nabla^\upsilon h\rangle = \langle(-1)^\upsilon div^\upsilon\phi, h\rangle.$$

We call $(-1)^\upsilon\ div^\upsilon\phi$ the υth fractional divergence of the gradient vector $\nabla^\upsilon\phi = (D_x^\upsilon\phi, D_y^\upsilon\phi)^T$.

From (14) and (15), we obtain

$$\begin{aligned}(-1)^\upsilon div^\upsilon\phi = &\sum_{k=0}^{N-1}(-1)^k \binom{\upsilon}{k} \phi_1(x+k,y) \\ &+ \sum_{k=0}^{N-1}(-1)^k \binom{\upsilon}{k} \phi_2(x,y+k),\end{aligned} \tag{17}$$

and with $\phi_1 = D_x^\upsilon\phi, \phi_2 = D_y^\upsilon\phi$.

B. FRACTIONAL DISTANCE REGULARIZATION TERM

As explained in Section *II.B*, LSEWR penalizes the deviation of the LSF and the signed distance function by the distance regularization term $E_{reg}(\phi)$. But when $|\nabla\phi| = 0$, its diffusion coefficient $d \to -\infty$, which will aggravate the irregularity of the LSF in a flat region.

To overcome this defect, here we propose a fractional distance regularization term, which makes the LSF ϕ approximate the signed distance function in the fractional dimension. In other words, this makes LSF meet $|\nabla^\upsilon\phi| \to 1$ during the evolution process, so as to ensure the LSF to evolve smoothly in steep areas and avoid the diffusion coefficient in flat areas becoming infinite. To this end, we define the following energy functional

$$E_{frac-reg} = \int_\Omega \frac{1}{2}(|\nabla^\upsilon\phi| - 1)^2 dxdy, \tag{18}$$

where $\upsilon \in R$ is a real number, and $|\nabla^\upsilon\phi|$ is the υth fractional gradient modular of the function ϕ. Obviously, when $|\nabla^\upsilon\phi| = 1$, the energy functional (18) reaches the minimum value. This makes the LSF move in a direction that satisfies $|\nabla^\upsilon\phi| \to 1$, thereby ensuring that the slope of the LSF will not be too steep during the evolution process. In fact, when the fractional order $\upsilon = 1$, (18) is simplified to (2), that is, (2) can be regarded as a special case of the fractional distance regularization term in this paper. Since the LSF ϕ is an approximation to the signed distance function in the fractional dimension, (18) has the same advantages as (2). Moreover, (18) makes the LSF not need to be initialized and periodically re-initialized to the signed distance function during the evolution. This greatly improves the efficiency of the model.

Next, we derive the level set evolution equation corresponding to (18) to further illustrate the advantages of the fractional distance regularization term. For formal simplicity, we denote

$$E_{Frac-reg} = \int_\Omega f(|\nabla^\upsilon\phi|)dxdy.$$

According to the basic principle of variational method, for any function $\eta \in C^\infty(\Omega)$, we define the value function of E_{Frac_reg} as

$$F(\lambda) = \int_\Omega f(|\nabla^\upsilon\phi + \lambda\nabla^\upsilon\eta|)dxdy,$$

where $\lambda > 0$ is a positive parameter. Then

$$\begin{aligned}\frac{dF(0)}{d\lambda} &= \lim_{\lambda\to 0}\frac{d}{d\lambda}\int_\Omega f(|\nabla^\upsilon\phi + \lambda\nabla^\upsilon\eta|)dxdy \\ &= \int_\Omega f'(|\nabla^\upsilon\phi|)\left(\frac{D_x^\upsilon\phi}{|\nabla^\upsilon\phi|}D_x^\upsilon\eta + \frac{D_y^\upsilon\phi}{|\nabla^\upsilon\phi|}D_y^\upsilon\eta\right)dxdy.\end{aligned}$$

Set $f(x) = \frac{1}{2}(x-1)^2$, we have $f'(|\nabla^\upsilon\phi|) = |\nabla^\upsilon\phi| - 1$, and so

$$\begin{aligned}\frac{dF(0)}{d\lambda} &= \int_\Omega \frac{(|\nabla^\upsilon\phi| - 1)D_x^\upsilon\phi}{|\nabla^\upsilon\phi|}\cdot D_x^\upsilon\eta dxdy \\ &\quad + \int_\Omega \frac{(|\nabla^\upsilon\phi| - 1)D_y^\upsilon\phi}{|\nabla^\upsilon\phi|}\cdot D_y^\upsilon\eta dxdy \\ &= \int_\Omega D_x^{\upsilon*}\left((1 - \frac{1}{|\nabla^\upsilon\phi|})D_x^\upsilon\phi\right)\cdot\eta dxdy \\ &\quad + \int_\Omega D_y^{\upsilon*}\left((1 - \frac{1}{|\nabla^\upsilon\phi|})D_y^\upsilon\phi\right)\cdot\eta dxdy.\end{aligned}$$

This gives the Euler-Lagrange equation of the energy functional (18)

$$D_x^{\upsilon*}\left((1 - \frac{1}{|\nabla^\upsilon\phi|})D_x^\upsilon\phi\right) + D_y^{\upsilon*}\left((1 - \frac{1}{|\nabla^\upsilon\phi|})D_y^\upsilon\phi\right) = 0.$$

Combining the definition of fractional divergence, we have

$$(-1)^\upsilon div^\upsilon\left((1 - \frac{1}{|\nabla^\upsilon\phi|})\nabla^\upsilon\phi\right) = 0.$$

Using the gradient descent method, the level set evolution equation corresponding to (18) is

$$\frac{\partial\phi}{\partial t} = -(-1)^\upsilon div^\upsilon\left((1 - \frac{1}{|\nabla^\upsilon\phi|})\nabla^\upsilon\phi\right). \tag{19}$$

Set $d^\upsilon = 1 - 1/|\nabla^\upsilon\phi|$ which is the fractional diffusion coefficient of equation (19).

Here we analyze the trend of the LSF from the value of d^{υ}. When $|\nabla^{\upsilon}\phi| > 1$, $d^{\upsilon} > 0$, the LSF diffuses forward. It reduces the slope of the LSF ϕ, so that the steep slope area of the function gradually slows down. When it falls to $|\nabla^{\upsilon}\phi| = 1$, there is $d^{\upsilon} = 0$, and at this point the LSF stops moving. When $|\nabla^{\upsilon}\phi| < 1, d^{\upsilon} < 0$, the LSF diffuses backward. The LSF gradually increases the slope in the flat area until $|\nabla^{\upsilon}\phi| = 1$ stops moving. In other words, the LSF always moves in the direction that satisfies $|\nabla^{\upsilon}\phi| \to 1$ during the evolution process, thereby approaching the signed distance function in the fractional dimension. The speed of change of the function ϕ is further analyzed below. In the steep slope area of the function ϕ, there are $|\nabla^{\upsilon}\phi| \to +\infty$ and $d^{\upsilon} \to 1$, which ensure the smooth forward diffusion of the LSF, and slowly reduce the height. The question is whether the function ϕ will appear a sharp change in a flat region similar to LSEWR? If only from the perspective of calculation, when $|\nabla^{\upsilon}\phi| = 0|, d^{\upsilon} \to -\infty$, this will make the LSF change sharply in a flat area. In fact, this kind of problem rarely happens, mainly because the fractional derivative is very different from the integer order derivative. The integer order derivative is a local operator, and there is $|\nabla\phi| = 0$ in the flat region, which leads to $d \to -\infty$. The fractional derivative has non-local properties. It can be known from Subsection *II.A* that the function ϕ does not appear $|\nabla^{\upsilon}\phi| = 0$. It means that in the flat region $|\nabla^{\upsilon}\phi| \neq 0$, naturally, $d^{\upsilon} \to -\infty$ will not appear. In this way, the sharp reverse diffusion of the LSF in the flat area will be avoided, and a large number of peaks and valleys will not appear in the flat area, which guarantees the smooth evolution of the LSF. We will further demonstrate the superiority of fractional distance regularity over integer order distance regularity in numerical experiments in Subsection *V.A*.

C. FRACTIONAL REGULARIZED VARIATIONAL LEVEL SET MODEL FOR IMAGE SEGMENTATION

Since the fractional distance regularization term does not contain image information, it is impossible to segment the image target edge only with this term. In order to achieve image segmentation, the fractional distance regularization term need to be combined with an external energy term containing image information to form a variational level set model. For this, we propose the following energy functional

$$E_{frac}(\phi) = \mu E_{frac-reg}(\phi) + E^{*}_{ext}(\phi). \tag{20}$$

Among them, $E_{frac-reg}(\phi)$ is (18), and its role is to regularize the LSF ϕ. $E^{*}_{ext}(\phi)$ is the external energy term, which drives the evolution curve towards the target edge, thereby achieving image segmentation.

LSEWR uses the weighted length and weighted area to describe the external energy term $E_{ext}(\phi)$ (in (4)). Energy functional will force the evolution curve to move towards the minimum geodesic length and weighted area, so as to achieve image segmentation. This is a good method of the level set method for image segmentation. But the edge indicator function $g(|\nabla I_{\sigma}|)$ that controls the weighted length and weighted area is only related to the gradient modular of the image. It is a positive function that decreases monotonically. This makes the LSF only move in one direction, which leads to it sensitivity to the initial position of evolution. Different initial positions may lead to different segmentation results. To effectively segment the image target, the initial curve must be surrounded or placed inside the target. The inward or outward movement of the evolution curve is implemented by the positive or negative selection of the coefficient ν. But when the target crosses the image boundary or there are multiple targets in the image, it is difficult for the evolution curve to have a proper initial position.

Now we discuss the construction of the external energy term $E^{*}_{ext}(\phi)$. Considering that the second-order Laplace operator has different signs on both sides of the image edge, the level set evolution curve can be forced to move in different directions. So, we construct the function $h(\cdot)$ based on the Laplace operator

$$h(I_{\sigma}) = sign(\Delta G_{\sigma} * I)$$

to weight the area. Here Δ is a Laplace operator. Because the exponential function has non-linear characteristics and is more suitable for image feature description, we adopt the exponential edge stop function

$$g(|\nabla I_{\sigma}|) = \exp(-|\nabla G_{\sigma} * I|/4)$$

to weight the length. Thus, our external energy term is as follow

$$\begin{aligned} E^{*}_{ext}(\phi) &= \lambda L_g(\phi) + \nu A_h(\phi) \\ &= \lambda \int_{\Omega} g(|\nabla I_{\sigma}|)\delta_{\varepsilon}(\phi)|\nabla\phi| dxdy \\ &\quad + \nu \int_{\Omega} h(I_{\sigma}) H_{\varepsilon}(-\phi) dxdy. \end{aligned} \tag{21}$$

From (18), (20), and (21), our fractional distance regularized variational level set model $E_{frac}(\phi)$ has the following form

$$\begin{aligned} E_{frac}(\phi) &= \mu \int_{\Omega} \frac{1}{2}(|\nabla^{\upsilon}\phi| - 1)^2 dxdy \\ &\quad + \lambda \int_{\Omega} g(|\nabla I_{\sigma}|)\delta(\phi)|\nabla\phi| dxdy \\ &\quad + \nu \int_{\Omega} h(I_{\sigma}) H(-\phi) dxdy, \end{aligned} \tag{22}$$

where $\mu, \lambda, \nu > 0$ are all constants.

It can be known from the structure of $h(I_{\sigma})$ that $h(I_{\sigma})$ has the same sign as the Laplace operator on both sides of the edge of the image target, which forces the LSF to move up (down) inside (out) the target according to the nature of the image. The target contour is formed at the junction of positive and negative, thereby obtaining image segmentation results. Thus, our model $E_{frac}(\phi)$ can initialize the LSF more flexibly. For example, the LSF can be initialized to a constant value $\phi_0 = \gamma$ (γ is a constant). This also allows the LSF to evolve without an initial contour, eliminating the choice of position for the initial contour, and thus overcoming the

sensitivity of the initial position in LSEWR. Minimizing the energy functional $E_{frac}(\phi)$, we obtain its corresponding level set evolution equation

$$\begin{aligned}\frac{\partial\phi}{\partial t} &= -\mu\cdot(-1)^{\upsilon}div^{\upsilon}\left((1-\frac{1}{|\nabla^{\upsilon}\phi|})\nabla^{\upsilon}\phi\right)\\ &+\lambda\delta(\phi)div(g(|\nabla I_{\sigma}|)\frac{\nabla\phi}{|\nabla\phi|})\\ &+\nu\delta(\phi)h(I_{\sigma}).\end{aligned}\tag{23}$$

IV. NUMERICAL IMPLEMENTATION

A. COVERING TEMPLATES OF FRACTIONAL DERIVATIVE AND DERIVATIVE CONJUGATE

To obtain the numerical approach of (23), we first give the numerical calculation of the fractional derivative D^{υ} and its conjugate $D^{\upsilon*}$. In (8), (9), (14), and (15), taking $k = 4$, we define the covering templates of the fractional derivatives D_x^{υ}, D_y^{υ} and their conjugates $D_x^{\upsilon*}$, $D_y^{\upsilon*}$ along the x-axis and y-axis directions respectively as Table 1.

B. NUMERICAL IMPLEMENTATION OF THE EVOLUTION EQUATION

The smooth Dirac function $\delta_{\varepsilon}(\phi)$ is defined as

$$\delta_{\varepsilon}(\phi)=\frac{1}{\pi}\cdot\frac{\varepsilon}{\varepsilon^2+x^2}.$$

Let the time step be Δt, the space step be h, $(x_i, y_i) = (ih, jh)$ be the spatial grid point, and $\phi_{i,j}^n$ be the state of function ϕ at (ih, jh) and time $t = n\Delta t$ $(n \geq 0)$. The time derivative on the left side of (23) is calculated by forward differences, the right fractional derivatives D_x^{υ}, D_y^{υ}, $D_x^{\upsilon*}$, and $D_y^{\upsilon*}$ by applying the covering templates in Table 1, and the integer order derivatives $D_x\phi_{i,j}$ and $D_y\phi_{i,j}$ by central differences, that is

$$D_x\phi_{i,j}=\frac{\phi_{i+1,j}-\phi_{i-1,j}}{2h},\quad D_y\phi_{i,j}=\frac{\phi_{i,j+1}-\phi_{i,j-1}}{2h}.$$

Thus, the discrete form of (23) is written as

$$\phi_{i,j}^{n+1}=\phi_{i,j}^n+\Delta tL(\phi_{i,j}^n),\tag{24}$$

where

$$\begin{aligned}L(\phi_{i,j}^n) &= -\mu l_{i,j}^n+\lambda\delta(\phi_{i,j}^n)D_x\left(g(|\nabla I_{\sigma}|)D_x(r_{i,j}^n)\right)\\ &+\lambda\delta(\phi_{i,j}^n)D_y\left(g(|\nabla I_{\sigma}|)D_y(r_{i,j}^n)\right)+\nu\delta(\phi_{i,j}^n)h(I_{\sigma}),\end{aligned}$$

and

$$\begin{aligned}l_{i,j}^n &= D_x^{\upsilon*}\left((1-\frac{1}{\sqrt{(D_x^{\upsilon}\phi_{i,j}^n)^2+(D_y^{\upsilon}\phi_{i,j}^n)^2}})D_x^{\upsilon}\phi_{i,j}^n\right)\\ &+D_y^{\upsilon*}\left((1-\frac{1}{\sqrt{(D_x^{\upsilon}\phi_{i,j}^n)^2+(D_y^{\upsilon}\phi_{i,j}^n)^2}})D_y^{\upsilon}\phi_{i,j}^n\right),\end{aligned}\tag{25}$$

TABLE 1. Covering templates of fractional derivative and the conjugate fractional derivative on x or y coordinates.

0	0	0	0	0	0	0	0	0
0	0	0	0	0	0	0	0	0
0	0	0	0	0	0	0	0	0
0	0	0	0	0	0	0	0	0
$\frac{\upsilon(\upsilon-1)(\upsilon-2)(\upsilon-3)}{24}$	$-\frac{\upsilon(\upsilon-1)(\upsilon-2)}{6}$	$\frac{\upsilon(\upsilon-1)}{2}$	$-\upsilon$	1	0	0	0	0
0	0	0	0	0	0	0	0	0
0	0	0	0	0	0	0	0	0
0	0	0	0	0	0	0	0	0
0	0	0	0	0	0	0	0	0

(a) D_x^{υ} covering template

0	0	0	0	0	0	0	0	0
0	0	0	0	0	0	0	0	0
0	0	0	0	0	0	0	0	0
0	0	0	0	0	0	0	0	0
0	0	0	0	1	0	0	0	0
0	0	0	0	$-\upsilon$	0	0	0	0
0	0	0	0	$\frac{\upsilon(\upsilon-1)}{2}$	0	0	0	0
0	0	0	0	$-\frac{\upsilon(\upsilon-1)(\upsilon-2)}{6}$	0	0	0	0
0	0	0	0	$\frac{\upsilon(\upsilon-1)(\upsilon-2)(\upsilon-3)}{24}$	0	0	0	0

(b) D_y^{υ} covering template

0	0	0	0	0	0	0	0	0
0	0	0	0	0	0	0	0	0
0	0	0	0	0	0	0	0	0
0	0	0	0	0	0	0	0	0
0	0	0	0	1	$-\upsilon$	$\frac{\upsilon(\upsilon-1)}{2}$	$-\frac{\upsilon(\upsilon-1)(\upsilon-2)}{6}$	$\frac{\upsilon(\upsilon-1)(\upsilon-2)(\upsilon-3)}{24}$
0	0	0	0	0	0	0	0	0
0	0	0	0	0	0	0	0	0
0	0	0	0	0	0	0	0	0
0	0	0	0	0	0	0	0	0

(c) $D_x^{\upsilon*}$ covering template

0	0	0	0	0	0	0	0	0
0	0	0	0	0	0	0	0	0
0	0	0	0	0	0	0	0	0
0	0	0	0	0	0	0	0	0
0	0	0	0	1	0	0	0	0
0	0	0	0	$-\upsilon$	0	0	0	0
0	0	0	0	$\frac{\upsilon(\upsilon-1)}{2}$	0	0	0	0
0	0	0	0	$-\frac{\upsilon(\upsilon-1)(\upsilon-2)}{6}$	0	0	0	0
0	0	0	0	$\frac{\upsilon(\upsilon-1)(\upsilon-2)(\upsilon-3)}{24}$	0	0	0	0

(d) $D_y^{\upsilon*}$ covering template

$$g(|\nabla I_{\sigma}|)=\exp\left(-\sqrt{D_x(G_{\sigma}*I))^2+(D_y(G_{\sigma}*I)/4}\right),\tag{26}$$

$$h(I_{\sigma})=sign\left(D_x(D_x(G_{\sigma}*I))+D_y(D_y(G_{\sigma}*I))\right),\tag{27}$$

$$r_{i,j}^n=\frac{\phi_{i,j}^n}{\sqrt{(D_x\phi_{i,j}^n)^2+(D_y\phi_{i,j}^n)^2}}.\tag{28}$$

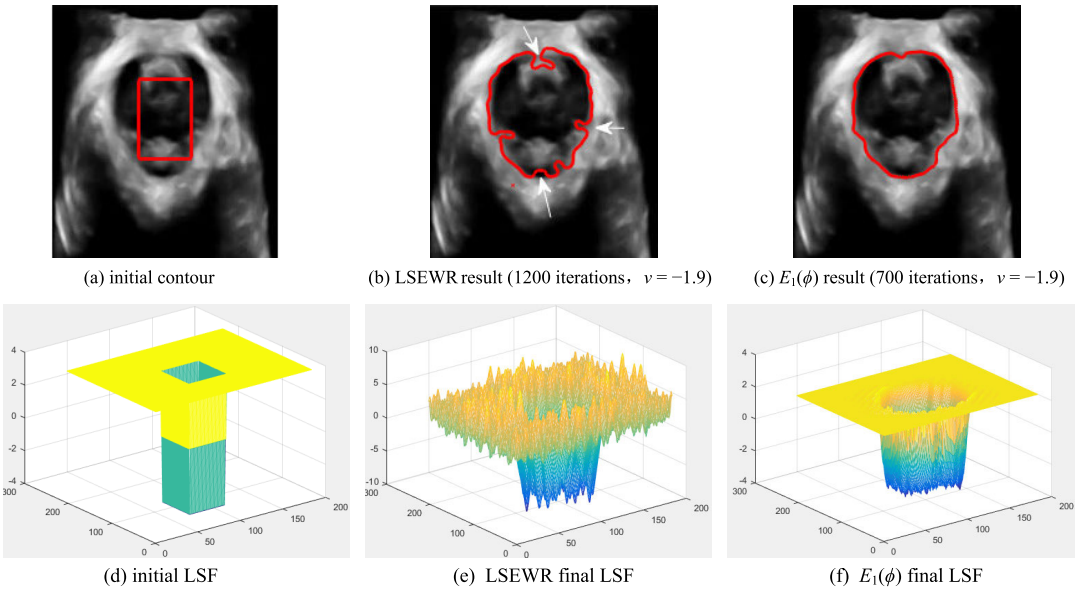

(a) initial contour (b) LSEWR result (1200 iterations, $v=-1.9$) (c) $E_1(\phi)$ result (700 iterations, $v=-1.9$)

(d) initial LSF (e) LSEWR final LSF (f) $E_1(\phi)$ final LSF

FIGURE 1. Evaluation of the effect of fractional distance regularization.

The procedures of the proposed algorithm are summarized as follows:

a) At $n=0$, the initial LSF is defined as $\phi_0=\gamma$ constant;

b) Calculating $g(|\nabla I_\sigma|)$ and $h(I_\sigma)$ according to (26) and (27);

c) Calculating $l_{i,j}^k$ and $r_{i,j}^k$ as in (25) and (28);

d) Iteratively solving (24) and updating the LSF to obtain ϕ^{n+1};

e) Checking whether the evolution curve converges. If not, go to step c); otherwise, stop the evolution.

V. EXPERIMENTAL RESULTS

This section includes two parts. In Subsection *A*, we compare the fractional distance regularity with the integer order distance regularity from numerical experiments. In Subsection *B*, we compare the image segmentation effect of our model $E_{frac}(\phi)$ with other models. The experimental platform operating system is Windows 10, and the codes is written in MATLAB R2016a.

A. EVALUATION OF FRACTIONAL DISTANCE REGULARIZATION

Here we combine our fractional distance regularization term with the external energy term in LSEWR [6] to evaluate the robustness of the fractional distance regularization term, namely

$$E_1(\phi)=\mu E_{frac\_reg}(\phi)+E_{ext}(\phi), \tag{29}$$

where $E_{frac\_reg}(\phi)$ is as in (18). The corresponding evolution equation is

$$\frac{\partial\phi}{\partial t}=-\mu\cdot(-1)^{\upsilon}div^{\upsilon}\left((1-\frac{1}{|\nabla^{\upsilon}\phi|})\nabla^{\upsilon}\phi\right)+\lambda\delta_\varepsilon(\phi)div(g(|\nabla I_\sigma|)\frac{\nabla\phi}{|\nabla\phi|})+\nu\delta_\varepsilon(\phi)g(|\nabla I_\sigma|) \tag{30}$$

The LSEWR model is as in (6)

$$\frac{\partial\phi}{\partial t}=\mu div\left((1-\frac{1}{|\nabla\phi|})\nabla\phi\right)+\lambda\delta_\varepsilon(\phi)div(g(|\nabla I_\sigma|)\frac{\nabla\phi}{|\nabla\phi|})+\nu\delta_\varepsilon(\phi)g(|\nabla I_\sigma|).$$

With the same external energy term, the evolution results of $E_1(\phi)$ and the LSEWR model are compared. The level set evolution of the two is shown in Figure 1 and Figure 2 respectively.

For fairness, the $E_1(\phi)$ and LSEWR model adopt the same binary function as the initial LSF, that is

$$\phi_0=\begin{cases}-4, & (x,y)\in\Omega_0\\ 4, & (x,y)\in\Omega-\Omega_0\end{cases}$$

and the same initial contour. Following experimental parameters in [6], $\mu=0.04$, $\lambda=5$, $\varepsilon=1.5$, $\sigma=1.2$, ν adjusted with different subjects, and $\upsilon=0.5$. The subject is an image of pelvic floor levator hiatus in ultrasound.

Figure 1 and Figure 2 show the evolution results of the $E_1(\phi)$ and LSEWR. The first line shows the initial contour, LSEWR segmentation result, and our $E_1(\phi)$ segmentation result. The second line shows the 3D displays of the initial LSF, the LSEWR final LSF, and the $E_1(\phi)$ final LSF. Experiments show that although the LSEWR model extracts or partially extracts the edge of the pelvic floor levator hiatus, the segmentation result is not accurate (see Figure 1 (b), indicated by the arrow). The LSF is trapped in a local minimum in a narrow area (see Figure 2 (b), the narrow part of the pelvic floor levator hiatus). There are many wave peaks and valleys in the flat area (see Figure 1 (e) and Figure 2 (e)), which indicates that the evolution of the LSF under the control of the integer order distance regularization term will violently

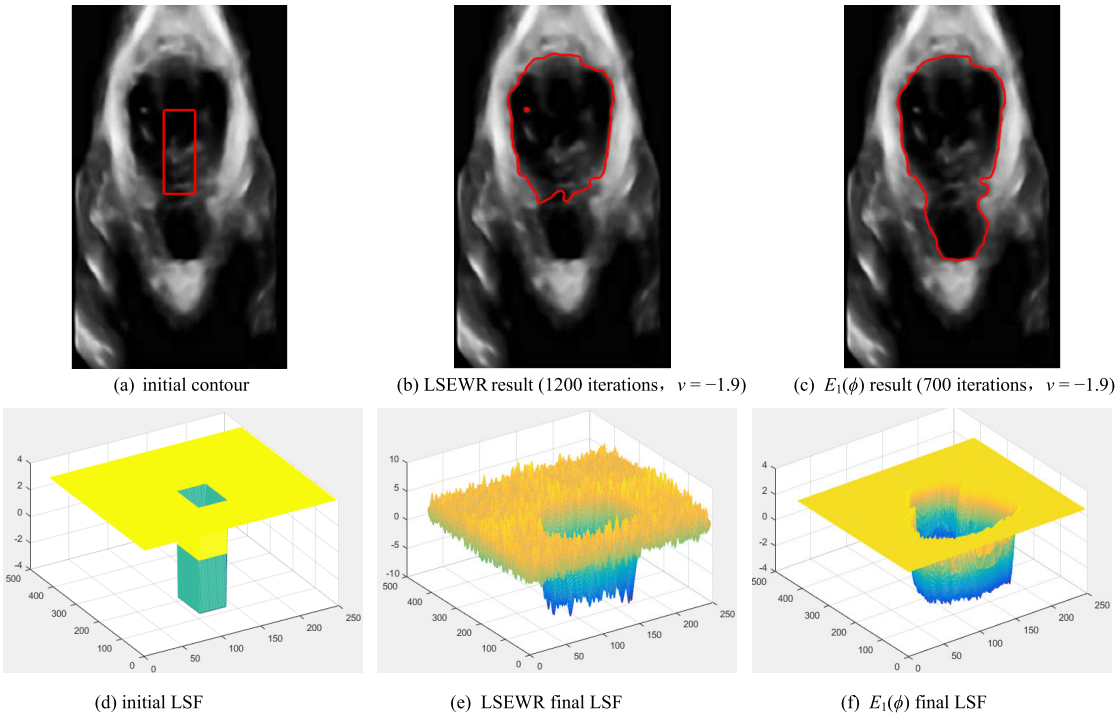

(a) initial contour (b) LSEWR result (1200 iterations, $v = -1.9$) (c) $E_1(\phi)$ result (700 iterations, $v = -1.9$)

(d) initial LSF (e) LSEWR final LSF (f) $E_1(\phi)$ final LSF

FIGURE 2. Evaluation of the effect of fractional distance regularization.

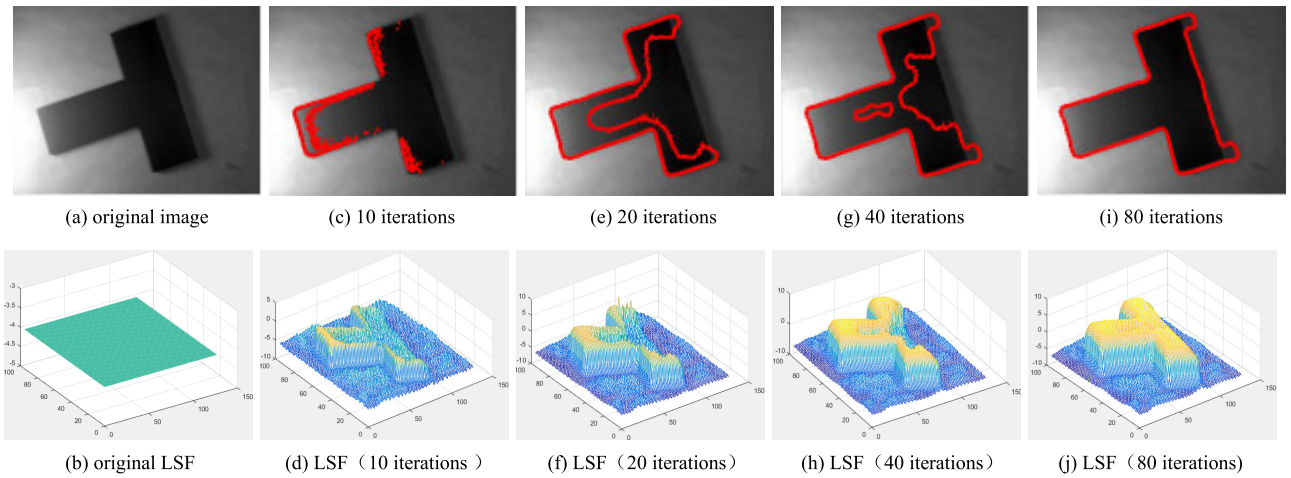

(a) original image (c) 10 iterations (e) 20 iterations (g) 40 iterations (i) 80 iterations

(b) original LSF (d) LSF（10 iterations） (f) LSF（20 iterations） (h) LSF（40 iterations） (j) LSF（80 iterations）

FIGURE 3. Segmentation processes of our model $E_{frac}(\phi)$.

oscillate in the flat region. This inevitably leads to inaccurate segmentation results. Given the same initial contour, with the same initial contour, our model $E_1(\phi)$ accurately extracted the edge of the pelvic floor levator hiatus (see Figure 1 (c) and Figure 2 (c)). The LSF is still flat and smooth in the flat area of the image (see Figure 1(f) and Figure 2 (f)), which illustrates the fractional distance regularization term has stronger regularity than the integer order regularization term. From the above, it can be seen that our fractional distance regularized model guarantees the smooth change of the LSF, so that it can segment the target edges more accurately.

B. EVALUATION OF OUR MODEL

In this subsection, experiments are performed on artificial and natural images to illustrate the effectiveness of our model $E_{frac}(\phi)$. The parameters in $E_{frac}(\phi)$ are selected as follows: $\sigma = 2.5$, $\varepsilon = 2.0$, $\mu = 0.04$, $\lambda = 5$, $\upsilon = 0.5$, time step $\Delta t = 5.0$, and the value of v varies with the experiment. The initial LSF $\phi_0 = 4$ or $\phi_0 = -4$. When the target is dark or black $\phi_0 = -4$, while bright $\phi_0 = 4$.

Figure 3 illustrates the image segmentation process of our model $E_{frac}(\phi)$ when the initial LSF is a constant function and $v = 1.5$. The experimental object is an artificial image with

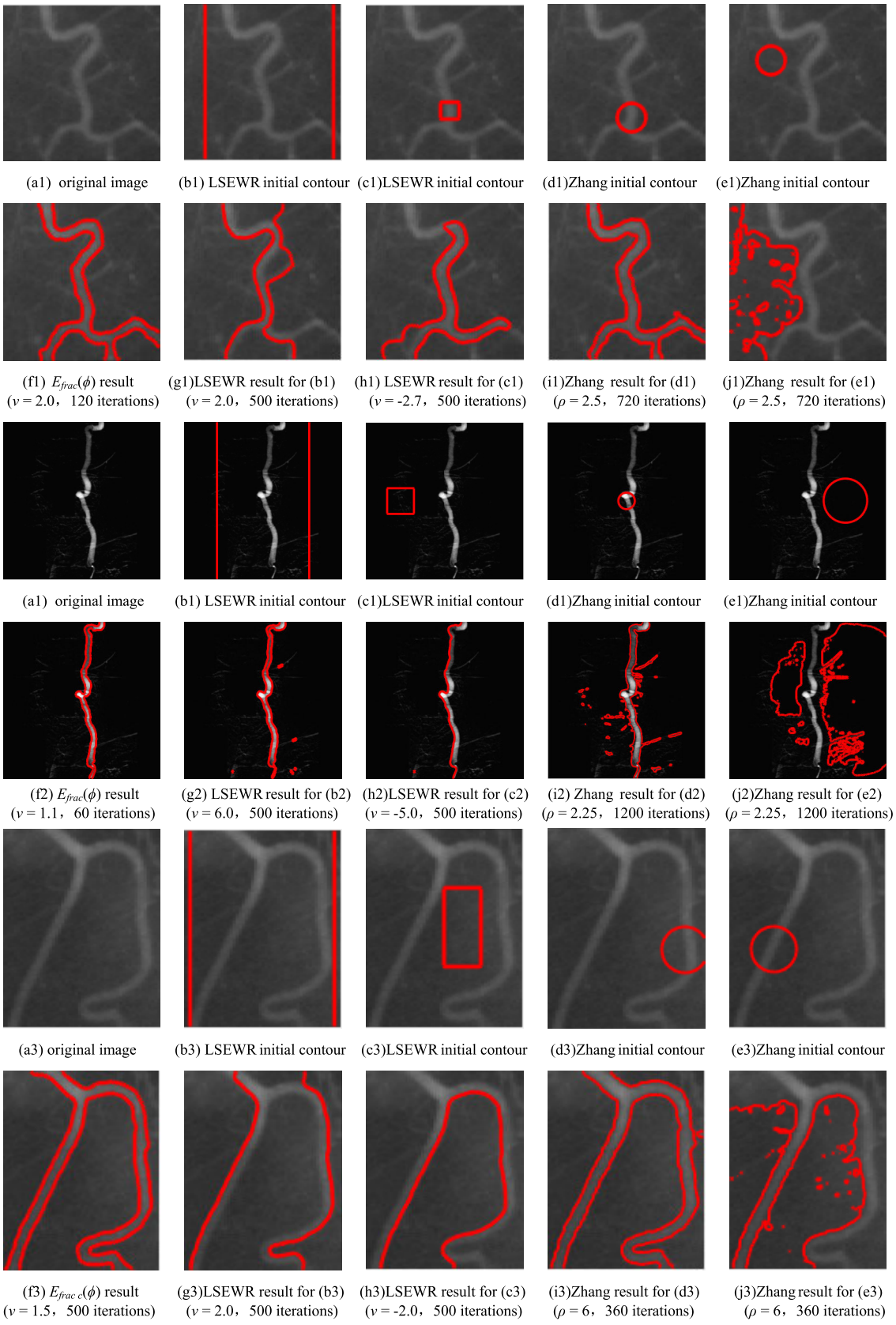

FIGURE 4. **Comparisons of the LSEWR model, Zhang model and our model E_{frac} (ϕ) for vessel images with intensity inhomogeneity.**

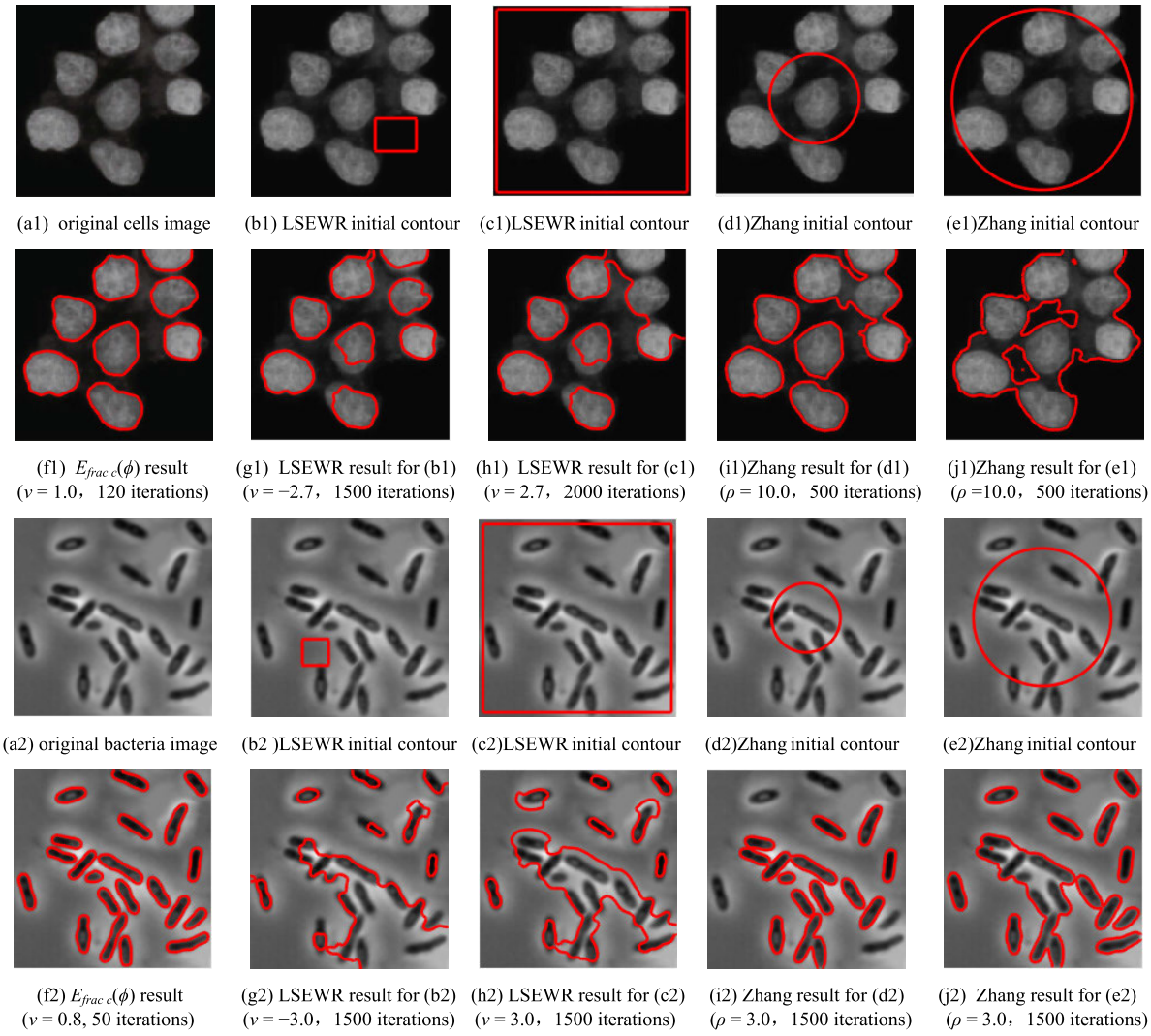

FIGURE 5. Comparisons of the LSEWR model, the Zhang mode and our model E_{frac} (ϕ) for images with multiple weak objects.

intensity inhomogeneity. The first line is the original image and curve evolution state, and the second line is the LSF evolution process. Initial LSF $\phi_0 = -4$ (see Figure 3 (b)), and there is no initial contour (see figure 3 (a)).

Affected by the external force of the image, the LSF gradually moves upwards inside the target area and downwards outside the target area. After 10 iterations, part of the LSF is above the zero level set (see Figure 3 (d)), and the contour of the left edge of the target begins to appear (Figure 3 (c)). After that, the LSF of the target area continue to rise (see figure 3(f), (h)), and the contour extended from left to right (figure 3(e), (g)). After 80 iterations, the LSF of the target area all exceeded the zero horizontal plane (Figure 3(j)), and the target edges were completely segmented (Figure 3 (i)). At this time, the LSF no longer changes, and the function converges between $[-10, 10]$. Experiments show that the LSF changes smoothly and orderly throughout the evolution process, which illustrates the effectiveness of fractional regularization terms.

Now, the proposed model is compared with the LSEWR model and Zhang model [2]. The LSEWR model and the Zhang model were selected for comparison, mainly because the two models are typical representatives of the variational level set model and can effectively segment intensity inhomogeneous images. The parameters in the LSEWR and the Zhang model are as consistent as possible with the original literature. The parameters that need to be selected through repeated experiments are the weighted area coefficient ν in LSEWR, the width ρ of the kernel function K_ρ in Zhang model, and the weighted area coefficient ν of $E_{frac}(\phi)$.

Figure 4 shows the experimental results of the $E_{frac}(\phi)$, LSEWR and Zhang models on images with intensity inhomogeneity. It can be seen from columns 2-5 that both the LSEWR and the Zhang model are sensitive to the initial position of the evolution curve. Different initial positions will have different segmentation results. Only when the initial position is reasonable, can a relatively ideal segmentation result be obtained (see figure 4(i1), (g2) and (i3)).

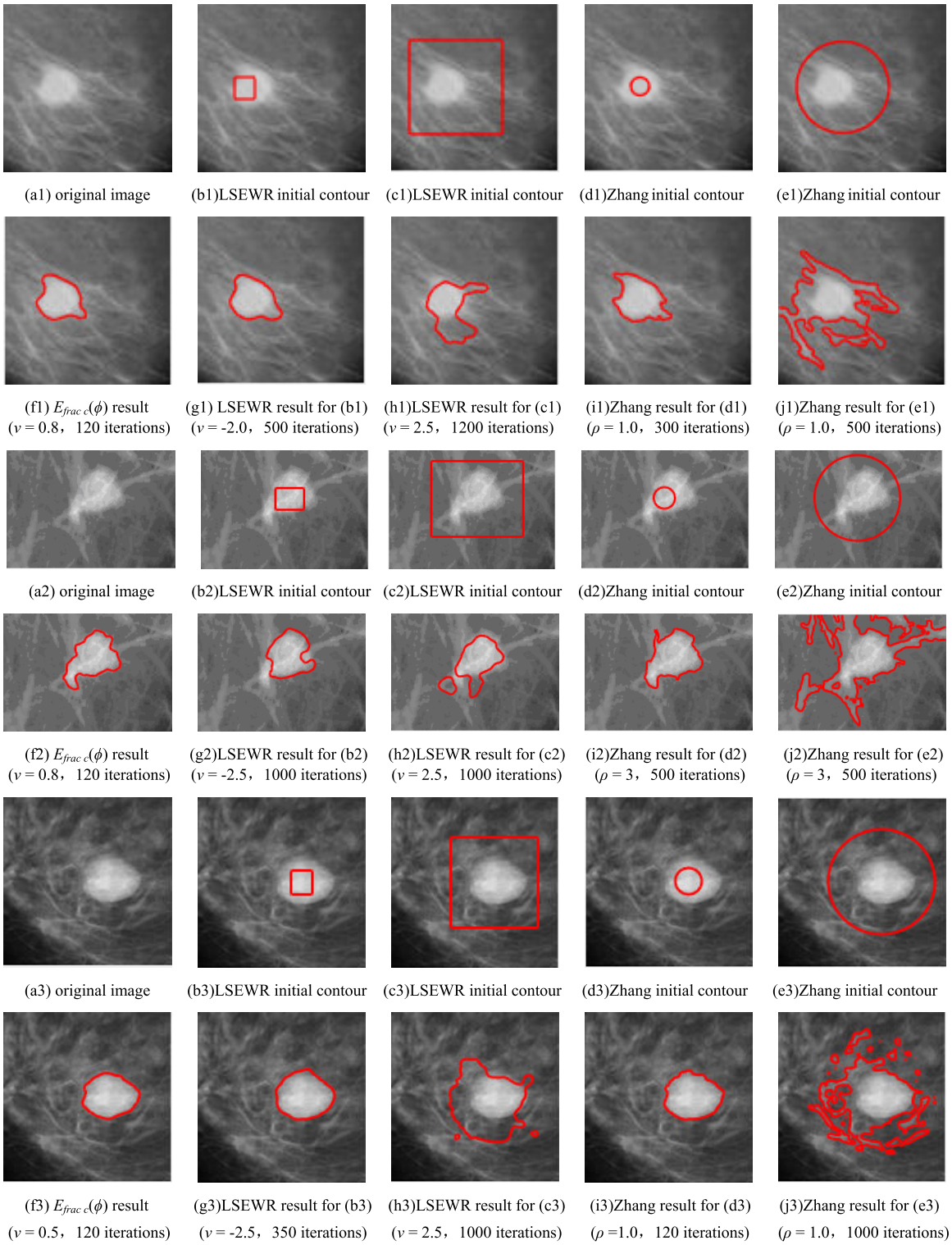

FIGURE 6. **Comparisons of the LSEWR model, the Zhang model and our model $E_{frac}(\phi)$ for breast cyst images.**

When the initial position is slightly changed, bad or even incorrect segmentation results will be produced (see Figure 4 (g1), (h1), (j1), (h2), (j2), (g3), (h3) and (j3)). And the segmentation results are sensitive to noise. As can be seen from the first column, the evolution of the model $E_{frac}(\phi)$ starts from $\phi_0 = 4$ with no initial contour, and the LSF adaptively moves up and down according to the image information. The experimental results show that the model in this paper can adaptively and accurately extract blood vessel edges (see Figure4 (f1) (f2) and (f3)). Some very

TABLE 2. Iterations and CPU time for the three models.

	Figure 4(a1)		Figure 4(a2)		Figure 4(a3)	
	iterations	time(s)	iterations	time(s)	iterations	time(s)
$E_{frac\ c}(\phi)$	120	4.3	60	4.7	500	11.5
LSEWR	500	36.6	500	43.2	500	35.1
Zhang	720	22.7	1200	125.2	360	41.7

weak blood vessel edges are also correctly extracted, and the segmentation results are not affected by noise.

Table 2 shows the final iterations and CPU time in this experiment of the $E_{frac}(\phi)$, LSEWR and Zhang model. The data shows that the convergence speed of the LSEWR model is 36.6, 43.2, and 35.1 seconds, which is 3-11 times the time consumed by the model in this paper. This is due to the sharp fluctuations in the level set evolution, which affect the evolution and convergence speed of the LSF, as seen in Figure 4. The Zhang model takes 22.7s, 125.2s, and 41.7s when it converges, which is 3-30 times longer than the model $E_{frac}(\phi)$ in this paper. The reason for time-consuming is that the algorithm is too complicated. It takes time for each evolution, and iterates multiple times to converge. Our model has simple calculation and stable evolution, so it can obtain the edge contour of the image at a faster speed, which only takes 4.3s, 4.7s, and 11.5s. Especially in Figure 4(a3), although the model $E_{frac}(\phi)$ has iterated 500 times, it takes less than 1/3 of the LSEWR model and the Zhang model, which shows the rapid effectiveness of the model.

Figure 5 shows the experimental results of the three models on multi-target intensity inhomogeneous images. The purpose of the experiment is to segment the cell and bacteria in the image (see Figure 5 (a1) and (a2)). Observing columns 2 and 3, although different initial contours are selected (outside the target or surrounding all targets), the LSEWR model still cannot successfully segment a single individual, as shown in the upper right corner of Figure 5 (h1)(the four targets), and in the middle of Figure 5 (g2), (h2)(multiple targets). The LSEWR model makes the curves mutually exclusive during the evolution process, gradually falling into a local minimum. Looking at columns 4 and 5, the Zhang model also fell into a local minimum when the evolution curve moved to a certain time (see Figure 5 (i1), (j1), and (j2)). And it cannot segment targets that are too far away from the initial contour (see Figure 5 (i2)). As can be seen from Figures 5 (f1) and (f2), in our model $E_{frac}(\phi)$, the LSF adaptively moves up and down according to the image information without the initial contour, automatically segmenting cells and bacteria from the background. It not only can accurately extract the edges of multi-targets, but also does not fall into the local minimum, which illustrates the effectiveness of the model in this paper for multi-target image segmentation.

Figure 6 shows the experimental results of the three models on breast cyst images. Due to the influence of noise such as hair follicles and villi, it is difficult to correctly segment breast cysts. The original image and the $E_{frac}(\phi)$ experimental results are in column 1, the LSEWR model in columns 2 and 3, and the Zhang model in columns 4 and 5. It can be seen from columns 2 and 4 that when the initial contour is inside the target, the LSEWR model and the Zhang model can obtain the target edge. But for images with irregular targets, the segmentation accuracy needs to be improved. As shown in Figure 6 (g2), the sharp corner of the left end of the target cannot be segmented by the LSEWR model. In Figure 6 (i2), the Zhang model segmented the target too much, so that the hair follicles at the edges of the target were extracted. From columns 3 and 5, when the initial contour is not inside the target and affected by noise such as villi, neither the LSEWR model nor the Zhang model can correctly segment breast cysts. Our model $E_{frac}(\phi)$ starts with $\phi_0 = -4$ and has no initial contour. The experimental results (column 1) show that the model $E_{frac}(\phi)$ can automatically and accurately segment breast cysts based on image information. The segmentation results are not affected by the noise of the hair follicle, which shows the effectiveness of the model in medical noise image segmentation.

VI. CONCLUSION

Using the definition of G-L fractional derivative, we derive the discrete form of the conjugate of fractional derivatives and fractional divergence. On this basis, we propose a variational level set model based on the fractional distance regularization term for image segmentation. The designed fractional distance regularization term guarantees that the LSF approximates the signed distance function in fractional order, thereby ensuring the accuracy of the LSF calculation and the stability and smoothness of the evolution. The constructed external energy term contains image gradient and Laplace operator information. It forces the LSF to adaptively move up and down according to the image information, and automatically generates contours to describe the edges of the image. The model allows the LSF to be simply initialized as a constant value function, greatly speeding up the convergence of the LSF. Experiments show that under the control of the fractional distance regularization term, our model can effectively segment weak intensity inhomogeneous targets and noisy medical images. The fractional regularization is a new research topic. In this paper, the stable evolution of the level set is studied under the framework of the fractional distance regularization. Our future work will focus on the convergence and stability of the fractional distance regularization algorithm and its application in other fields of the image processing, such as saliency detection, etc.

REFERENCES

[1] S. Osher and J. A. Sethian, "Fronts propagating with curvature-dependent speed: Algorithms based on Hamilton–Jacobi formulations," *J. Comput. Phys.*, vol. 79, no. 1, pp. 12–49, Nov. 1988.

[2] K. Zhang, L. Zhang, K.-M. Lam, and D. Zhang, "A level set approach to image segmentation with intensity inhomogeneity," *IEEE Trans. Cybern.*, vol. 46, no. 2, pp. 546–557, Feb. 2016.
[3] K. Hanbay and M. F. Talu, "A novel active contour model for medical images via the Hessian matrix and eigenvalues," *Comput. Math. Appl.*, vol. 75, no. 9, pp. 3081–3104, May 2018.
[4] L. Fang, W. Zhao, X. Li, and X. Wang, "A convex active contour model driven by local entropy energy with applications to infrared ship target segmentation," *Opt. Laser Technol.*, vol. 96, pp. 166–175, Nov. 2017.
[5] V. Caselles, F. Catté, T. Coll, and F. Dibos, "A geometric model for active contours in image processing," *Numerische Math.*, vol. 66, no. 1, pp. 1–31, Dec. 1993.
[6] C. Li, C. Xu, C. Gui, and M. D. Fox, "Level set evolution without re-initialization: A new variational formulation," in *Proc. IEEE Comput. Soc. Conf. Comput. Vis. Pattern Recognit. (CVPR)*, San Diego, CA, USA, vol. 1, Jun. 2005, pp. 430–436.
[7] C. Li, C. Xu, C. Gui, and M. D. Fox, "Distance regularized level set evolution and its application to image segmentation," *IEEE Trans. Image Process.*, vol. 19, no. 12, pp. 3243–3254, Dec. 2010.
[8] X. Wang, J. Shan, Y. Niu, L. Tan, and S.-X. Zhang, "Enhanced distance regularization for re-initialization free level set evolution with application to image segmentation," *Neurocomputing*, vol. 141, pp. 223–235, Oct. 2014.
[9] X.-F. Wang, H. Min, L. Zou, and Y.-G. Zhang, "A novel level set method for image segmentation by incorporating local statistical analysis and global similarity measurement," *Pattern Recognit.*, vol. 48, no. 1, pp. 189–204, Jan. 2015.
[10] Y. Pu, "Fractional calculus approach to texture of digital image," in *Proc. ICSP*, Beijing, China, vol. 2, Nov. 2006, pp. 16–20, doi: 10.1109/ICOSP.2006.345713.
[11] Y.-F. Pu, J.-L. Zhou, and X. Yuan, "Fractional differential mask: A fractional differential-based approach for multiscale texture enhancement," *IEEE Trans. Image Process.*, vol. 19, no. 2, pp. 491–511, Feb. 2010.
[12] Y. Zhang, H. D. Cheng, J. Tian, J. Huang, and X. Tang, "Fractional sub-pixel diffusion and fuzzy logic approach for ultrasound speckle reduction," *Pattern Recognit.*, vol. 43, no. 8, pp. 2962–2970, Aug. 2010.
[13] Z. Jun and W. Zhihui, "A class of fractional-order multi-scale variational models and alternating projection algorithm for image denoising," *Appl. Math. Model.*, vol. 35, no. 5, pp. 2516–2528, May 2011.
[14] B. Chen, S. Huang, Z. Liang, W. Chen, and B. Pan, "A fractional order derivative based active contour model for inhomogeneous image segmentation," *Appl. Math. Model.*, vol. 65, pp. 120–136, Jan. 2019.
[15] Z. Ren, "Adaptive active contour model driven by fractional order fitting energy," *Signal Process.*, vol. 117, pp. 138–150, Dec. 2015.
[16] A. Laghrib, A. Ben-Loghfyry, A. Hadri, and A. Hakim, "A nonconvex fractional order variational model for multi-frame image super-resolution," *Signal Process., Image Commun.*, vol. 67, pp. 1–11, Sep. 2018.
[17] K. B. Oldham and J. Spanier, *The Fractional Calculus Theory and Applications of Differentiation and Integration to Arbitrary Order*. New York, NY, USA: Academic, 1974.
[18] I. Podlubny, *Fractional Differential Equations*. New York, NY, USA: Academic, 1999.
[19] Y. Pu, W. Wang, J. Zhou, Y. Wang, and H. Jia, "Fractional differential approach to detecting textural features of digital image and its fractional differential filter implementation," *Sci. China F, Inf. Sci.*, vol. 51, no. 9, pp. 1319–1339, Sep. 2008.
[20] C. Ionescu and J. F. Kelly, "Fractional calculus for respiratory mechanics: Power law impedance, viscoelasticity, and tissue heterogeneity," *Chaos, Solitons Fractals*, vol. 102, pp. 433–440, Sep. 2017.
[21] J. Gomes and O. Faugeras, "Reconciling distance functions and level sets," *J. Vis. Commun. Image Represent.*, vol. 11, no. 2, pp. 209–223, Jun. 2000.
[22] V. I. Arnold, *Geometrical Methods in the Theory of Ordinary Differential Equations*. New York, NY, USA: Springer-Verlag, 1983.

MENG LI received the M.S. degree in applied mathematics and the Ph.D. degree in computational mathematics from Chongqing University, Chongqing, China, in 2008 and 2011, respectively. From March 2012 to November 2013, she was a Lecture with the Department of Mathematics, Chongqing University of Arts and Sciences. Since December 2013, she has been an Assistant Professor with the College of Mathematics and Statistics, Chongqing Technology and Business University, Chongqing. Her research interests include partial differential equation and image processing.

YI ZHAN received the M.S. degrees from the University of Chongqing, Chongqing, China, in 2006, and the Ph.D. degree from Sichuan University, Chengdu, China, in 2009.

From 2011 to 2014, he was a Postdoctoral Fellow with the School of Mathematics and Statistics, Chongqing University. Since 2012, he has been an Assistant Professor with the College of Mathematics and Statistics, Chongqing Technology and Business University. His research interests include partial differential equation image recovery, image reconstruction, nonlocal theory, and applied research.

YONGXIN GE received the B.Sc. degree in information and computing science, the M.Sc. degree in operations research and control theory, and the Ph.D. degree in computer science and technology from Chongqing University, Chongqing, China, in 2003, 2006, and 2011, respectively. He is currently an Associate Professor with the School of Big Data and Software Engineering, Chongqing University. His research interests include computer vision, patter recognition, and machine learning.